J Math Chem (2013) 51:1056–1075
DOI 10.1007/s10910-012-0137-0

ORIGINAL PAPER

A boundary-driven reaction front

J. H. Merkin

Received: 26 October 2012 / Accepted: 25 December 2012 / Published online: 4 January 2013
© Springer Science+Business Media New York 2013

Abstract A model reaction scheme in which two species A and B react to form an inert product is considered, with the possible linear decay of A to a further inert prduct also included. The reaction between A and B is maintained by the input of A from the boundary which keeps A at a constant concentration. The cases when B is immobile or free to diffuse are treated. In the former case reaction fronts in B are seen to develop. Large time asymptotic solutions are derived which show that these fronts propagate across the reactor at rates proportional to $t^{1/2}$ or $\log t$ (t is a dimensionless time) depending on whether the extra decay step is included. A similar situation is seen when B can diffuse when the linear decay step is not present. However, when this extra step is included in the reaction scheme the reaction zone reaches only a finite distance fronm the boundary at large times.

Keywords Quadratic reaction · Boundary input · Reaction fronts · Large time asymptotics

1 Introduction

Propagating reaction fronts play an important role in generating spatio-temporal structures in reaction–diffusion systems. Perhaps the most basic are those based on autocatalytic reactions whereby a reactant present initially is converted to an autocatalytic product, resulting in the development of a constant form travelling wave propagating with a constant speed. The Fisher–Kolmogorov wave [1,2] is a generic example, being based on quadratic autocatalysis, was the first to be studied in detail. This fundamental concept has been extended to systems based on cubic autocatalysis [3–5] and to more

J. H. Merkin (✉)
Department of Applied Mathematics, University of Leeds, Leeds LS2 9JT, UK
e-mail: amtjhm@maths.leeds.ac.uk

general orders of autocatalysis [6]. The inclusion of a terminating or decay step in the reaction scheme can substantially modify both the structure and propagation speed of the reaction front and can also lead to propagation inhibition [7,8].

Alternative mechanisms for the initiation of propagating reaction waves are based on excitable systems with perhaps the most studied being those based on the Belousov–Zhabotinsky reaction [9–11]. In these cases a sufficiently large perturbation to the uniform initial state is required to trigger propagation. This can, depending on the reaction kinetics, be either as a single pulse, where the system returns to its original state, or a propagating wave train, where the reaction is repeatedly fired. In higher dimensions this can lead to target patterns.

These previous studies have assumed an initial uniform distribution of the reactant with a perturbation to this state being made locally and the reaction wave then propagating away from this site. Here we consider a somewhat different situation whereby the propagation of the reaction front is maintained by the input of a reactant from the boundary. Our model has some similarities with catalyst pellets [12,13] where a reaction within the pellet can be sustained by conditions imposed on the boundary. However, our reaction scheme is basically different to those usually assumed for catalyst pellets, in that here we assume that the system is isothermal and that we have two reactants A and B (say) which react to form an inert product AB. We further assume the possibility of the reactant A being able to decay to another inert product. In other words our reaction scheme allows only for the depletion of both reactants A and B.

Initially we take the reaction region to be filled with the reactant B with the reaction initiated by the input of A from the boundary, which we assume to be a reservoir that can maintain reactant A at a constant concentration A_0 on the boundary. Our model is, to some extent, motivated by our previous work on the effects of a complexing agent on autocatalytic reaction fronts [14] and to this end we further assume that the reactant B is made up of large molecules relative those of A. This leads us to take B as either totally immobile or, if it can diffuse, to do so at a rate much slower than that of A. As a consequence of this, we take the reaction boundary to be impermeable to B.

Under these modelling assumptions we find that a reaction front in B can spread from the boundary. When B is assumed immobile, the rate of propagation depends on whether A decays or not. Without this extra decay step the propagation rate is proportional to $t^{1/2}$, where t is a (dimensionless) time, whereas with the decay step a constant concentration profile of A is attained at large times with a reaction with B spreading at a rate proportional to $\log t$. When B can diffuse, a similar situation is found when there is no decay of A. However, when A can also decay, steady profiles in both A and B are seen near the boundary with a diffusional spread of B further away from the boundary. We start by describing our model.

2 Model

Our model is based on the simple reaction whereby reactants A and B combine to form the product AB

$$A + B \rightarrow AB \quad \text{rate: } k_0\, ab \tag{1}$$

where a and b are respectively the concentrations of the reactants A and B and k_0 is a rate constant. We also assume that there can be a linear degradation of reactant A to an inert product

$$A \rightarrow \text{ Products} \quad \text{rate: } k_d\, a \tag{2}$$

We take planar geometry, with reactions (1, 2) then leading to the equations

$$\frac{\partial a}{\partial t} = D_A \frac{\partial^2 a}{\partial x^2} - k_0 ab - k_d a \tag{3}$$

$$\frac{\partial b}{\partial t} = D_B \frac{\partial^2 b}{\partial x^2} - k_0 ab \tag{4}$$

where D_A and D_B are respectively the diffusion coefficients of the reactants A and B and x is our spatial variable.

We assume that initially there is no reactant A present within the reaction domain which is filled only with the reactant B at a constant concentration B_0. The reactant A is supplied from a reservoir that can maintain a constant concentration A_0 at the boundary of the reactor. Both B and the product AB are assumed to be large molecules compared to the reactant A thus it is reasonable to assume that the reactor boundary is impermeable to B. This leads to the initial and boundary conditions

$$a = 0,\ b = B_0 \quad \text{at } t = 0 \quad (0 < x < \infty) \tag{5}$$

$$a = A_0, \quad \frac{\partial b}{\partial x} = 0 \quad \text{at } x = 0 \quad (t > 0) \tag{6}$$

We can make Eqs. (3–4) dimensionless by writing

$$a = A_0 \overline{a}, \quad b = B_0 \overline{b}, \quad \overline{t} = (k_0 A_0) t, \quad \overline{x} = x \left(\frac{k_0 A_0}{D_A} \right)^{1/2} \tag{7}$$

Then, on dropping the bars for convenience, this gives the dimensionless reaction–diffusion equations for our model as

$$\frac{\partial a}{\partial t} = \frac{\partial^2 a}{\partial x^2} - \delta ab - \beta a \tag{8}$$

$$\frac{\partial b}{\partial t} = D \frac{\partial^2 b}{\partial x^2} - ab \tag{9}$$

on $0 < x < \infty$, $t > 0$, with

$$a = 1, \ \frac{\partial b}{\partial x} = 0 \quad \text{at } x = 0 \quad (t > 0), \qquad b = 1,\ a = 0 \quad \text{at } t = 0 \quad (0 < x < \infty) \tag{10}$$

We apply the further condition that

$$\frac{\partial a}{\partial x} \to 0, \quad \frac{\partial b}{\partial x} \to 0 \quad \text{as } x \to \infty \quad (t > 0) \tag{11}$$

The dimensionless parameters in Eqs. (8, 9) are defined as

$$\delta = \frac{B_0}{A_0}, \quad \beta = \frac{k_d}{k_0 A_0}, \quad D = \frac{D_B}{D_A}$$

The parameter β gives a measure of the rate of degradation of the reactant, δ is a dimensionless measure of the the initial concentration of the reactant B relative to A and D is the ratio of the diffusion coefficients.

A basic assumption behind our model is that the reactant B is relatively immobile relative to the reactant A resulting in the diffusion coefficient ratio D being small. We start our discussion of the problem given by Eqs. (8, 9) subject to (10, 11) by considering the case when B is totally immobile, i.e. taking $D = 0$, treating first the case when there is no reactant degradation, $\beta = 0$. We then discuss the cases when there is reactant degradation, $\beta > 0$, and when the reactant B can diffuse, $D > 0$.

3 Reactant B immobile, D = 0

3.1 No reactant degradation, $\boldsymbol{\beta = 0}$

We note that, in this case, $b = \mathrm{e}^{-t}$ on $x = 0$. The problem given by (8–11) was solved numerically using the same technique that we have used previously for solving this type of reaction–diffusion problem, see [15–17] for example. The only difference being that here we used a predictor–corrector method to solve the ordinary differential equation that results when D is put to zero in Eq. (9). Our numerical solutions for this case show that the reactant A starts to spread across the reactor from the boundary input and continues to spread further as time increases. A front develops in B which also spreads from the boundary and in which b changes from zero (fully reacted) to its initial state ($b = 1$) over a relatively narrow region. It is in this thin region where reaction (1) takes place with this reaction zone moving further from the boundary as t increases. We illustrate this behaviour in Fig. 1 where we give profile plots of a and b for $\delta = 1.0$ (similar behaviour was found for other values of δ tried). We describe this movement of the reaction zone by calculating x_s, the position where $b = 0.5$, and I_a, the total amount of A produced at a given time. These are plotted against t in Fig. 2a where we see that they both increase monotonically with t.

3.1.1 Asymptotic solution for **t** *large*

The profile plots shown in Fig. 1 indicate that, for t large, there are two regions, an inner (fully reacted) region $0 \le x < c(t)$, with $c(t)$ increasing with t and to be determined, in which $b = 0$ and a decreases from its boundary value and a front (reaction) region,

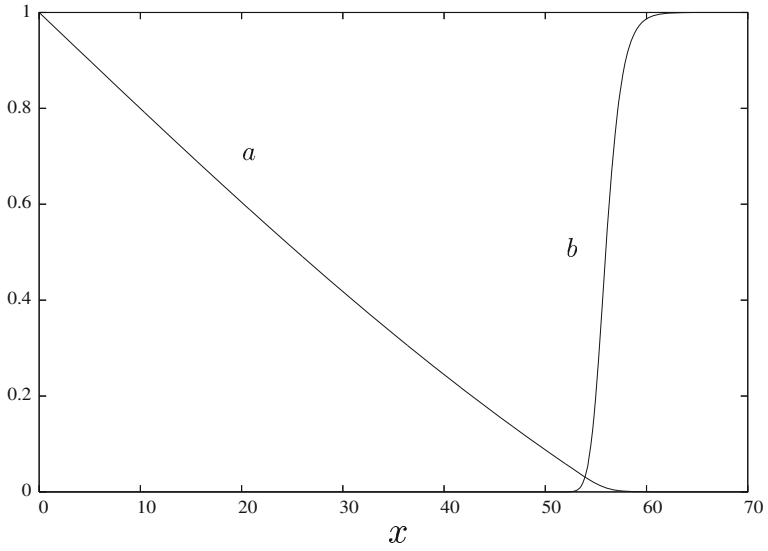

Fig. 1 Concentration profiles of A and B calculated from a numerical integration of equations (8, 9) subject to (10, 11) for $\delta = 1.0$, $\beta = 0.0$ and $D = 0$ at time $t = 2056.5$

where a is small and b changes to its outer value $b = 1$. In the inner region we put $\eta = x/c(t)$ and, with $b = 0$, we obtain from Eq. (8)

$$\frac{\partial^2 a}{\partial \eta^2} + (c\,\dot{c})\,\eta\,\frac{\partial a}{\partial \eta} = c^2\,\frac{\partial a}{\partial t} \tag{12}$$

Equation (12) requires that $(c\,\dot{c})$ be a constant for t large, which leads us to look for a solution of equation (12) by expanding

$$c(t) = 2c_0 t^{1/2} + \cdots, \quad a(\eta, t) = a_0(\eta) + \cdots \tag{13}$$

The leading-order behaviour, given by

$$a_0'' + 2c_0^2\,\eta\,a_0' = 0, \quad a_0(0) = 1 \tag{14}$$

where primes denote differentiation with respect to η. We solve (14) subject to the condition that $a_0(1) = 0$, i.e. $a = 0$ at $x = c(t)$ to leading order, finding

$$a_0 = 1 - \frac{1}{I_0}\int_0^{\eta} \mathrm{e}^{-c_0^2 s^2}\,ds \tag{15}$$

where

$$I_0(c_0) = \int_0^1 \mathrm{e}^{-c_0^2 s^2}\,ds = \frac{1}{c_0}\int_0^{c_0} \mathrm{e}^{-s^2}\,ds$$

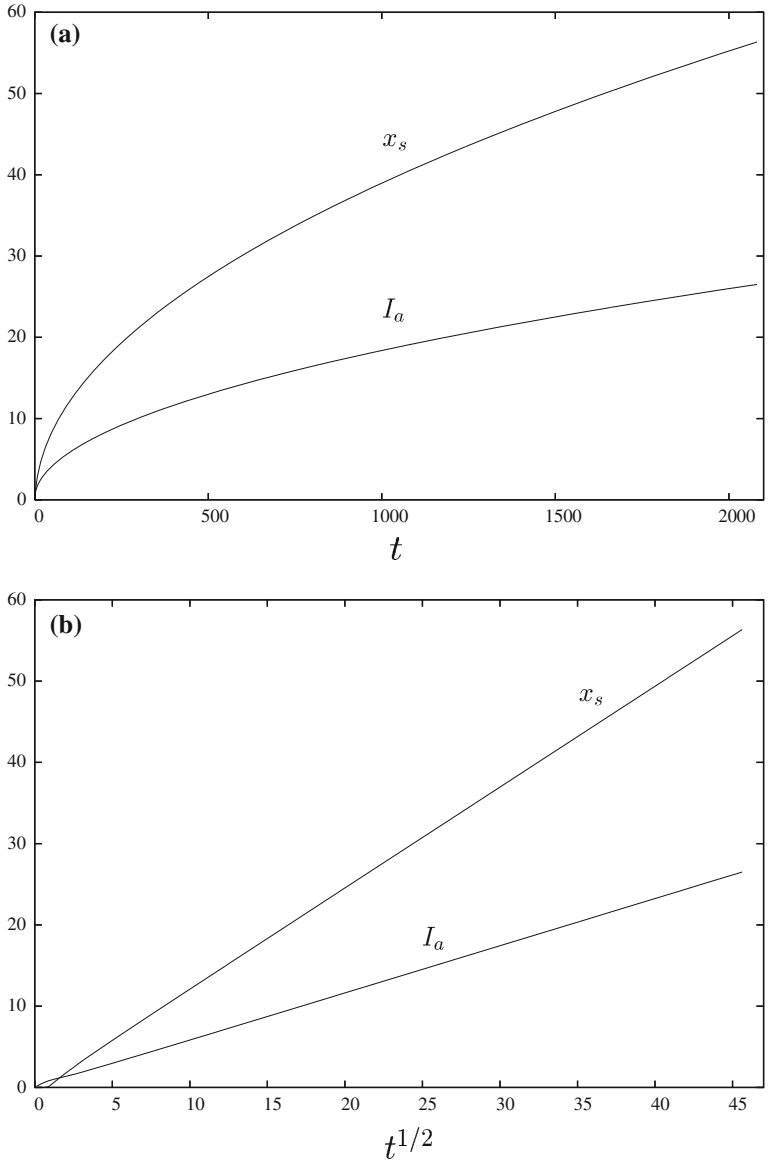

Fig. 2 *Plots* of the position of the reaction x_s and the amount of A formed I_a against **a** t and **b** $t^{1/2}$ for $\delta = 1.0$, $\beta = 0.0$ and $D = 0$

From (15), $a \sim d_0(1-\eta) + \cdots$ as $\eta \to 1$ from below, where $d_0 = \mathrm{e}^{-c_0^2}/I_0$. This suggests that, for the reaction region, we put

$$x = \overline{x} + c(t) = \overline{x} + 2c_0 t^{1/2} + \cdots, \quad a = t^{-1/2} f(\overline{x}, t) \tag{16}$$

Applying (16) in Eqs. (8, 9) then gives

$$(c_0 + \cdots)\frac{\partial b}{\partial \overline{x}} - fb = t^{1/2}\frac{\partial b}{\partial t}$$
$$\frac{\partial^2 f}{\partial \overline{x}^2} - \delta f b = \frac{\partial f}{\partial t} - t^{-1/2}(c_0 + \cdots)\frac{\partial f}{\partial \overline{x}} - \frac{1}{2}t^{-1} f \tag{17}$$

subject to, on matching with the inner region,

$$b \to 0,\ f \sim -\frac{d_0}{2c_0}\,\overline{x} + \cdots \text{ as } \overline{x} \to -\infty, \quad f \to 0,\ b \to 1 \quad \text{as } \overline{x} \to \infty \tag{18}$$

The leading-order problem is

$$c_0 b' - fb = 0, \quad f'' - \delta f b = 0 \tag{19}$$

where primes now denote differentiation with respect to $\overline{x}$. We can combine equations (19), integrate and apply the conditions as $\overline{x} \to \infty$ to obtain

$$f' + \delta c_0 (1 - b) = 0 \tag{20}$$

Applying the conditions as $\overline{x} \to -\infty$ then gives

$$-\frac{d_0}{2c_0} + \delta c_0 = 0, \quad \text{or} \quad \delta = \frac{\mathrm{e}^{-c_0^2}}{2c_0^2 I_0(c_0)} \tag{21}$$

Expression (21) is an implicit relation for c_0 in terms of δ. A graph of c_0 plotted against δ obtained from (21) is shown in Fig. 3. This shows that c_0 decreases as δ is increased, having $c_0 \sim (2\delta)^{-1/2} + \cdots$ for δ large.

Our asymptotic theory shows that, at large times, the inner region and the reaction zone spread from the boundary at rate proportional to $t^{1/2}$ and that the reaction zone, in which A reacts with B has as an $O(1)$ thickness with the concentration of A being small, of $O(t^{-1/2})$. From (13), $x_s \sim 2c_0 t^{1/2} + \cdots$ and from (15) $I_a \sim \dfrac{(1 - \mathrm{e}^{-c_0^2})}{c_0 I_0}\, t^{1/2} + \cdots$. As a check on this behaviour we plot x_s and I_a obtained from our numerical integration for $\delta = 1.0$ against $t^{1/2}$ in Fig. 2b. We see that both plots give straight line behaviour for the larger values of t. Also, for $\delta = 1.0$, we find that Eq. (21) gives $c_0 = 0.62006$, consistent with the slope of $2c_0$ for x_s shown in Fig. 2b.

We next consider the case when the reactant A can be degraded through reaction (14), i.e. the case when $\beta \neq 0$. We still assume that the reactant B is immobile, $D = 0$.

3.2 Reactant degradation, $\boldsymbol{\beta \neq 0}$

In this case the concentration of reactant A approaches a steady state as t increases. A front in the reactant B again forms in which b changes from its fully reacted state, $b = 0$, to it initial state, $b = 1$, over a relatively narrow region. This front propagates

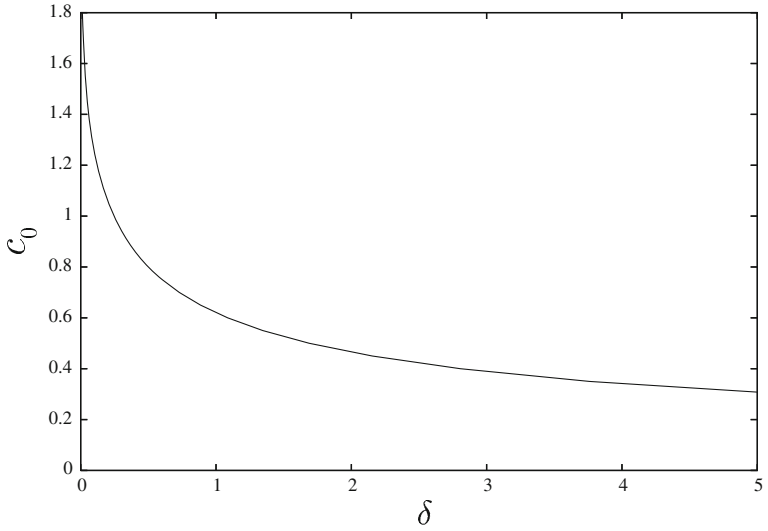

Fig. 3 A *plot* of c_0 against δ given by Eq. (21), the position of the reaction zone $x_s \sim 2c_0 t^{1/2}$ for t large

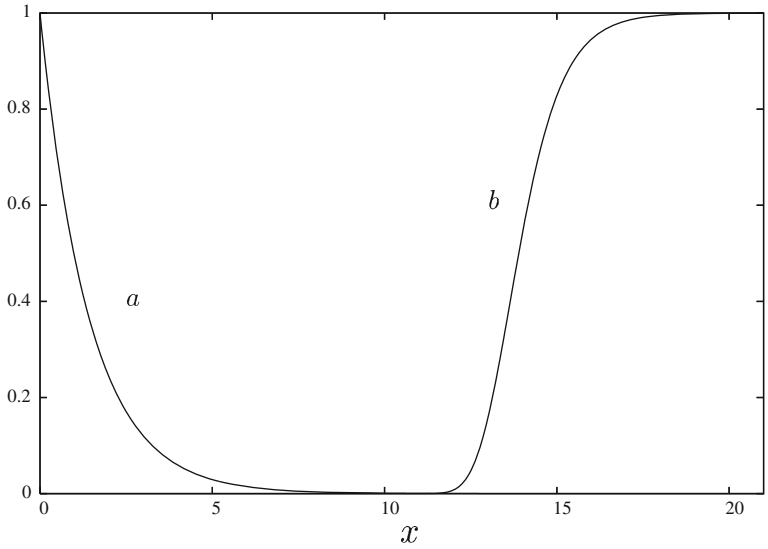

Fig. 4 Concentration profiles of A and B calculated from a numerical integration of equations (8, 9) subject to (10, 11) for $\delta = 1.0$, $\beta = 0.5$ and $D = 0$ at time $t = 32{,}250$

very slowly from the boundary. We illustrate this in Fig. 4 with profile plots of A and B for $\beta = 0.5$ and $\delta = 1.0$. We see that the two profiles have become largely separated from each other at this large time. To show that the concentration of A approaches a steady state we plot I_a against $\log t$ in Fig. 5a for representative values of β and again for $\delta = 1.0$, where we see that I_a approaches a constant value, dependent on β, as t increases. The rate of approach to this steady state becomes slower as the value of β is decreased, as might be expected. To indicate how the front in B propagates we

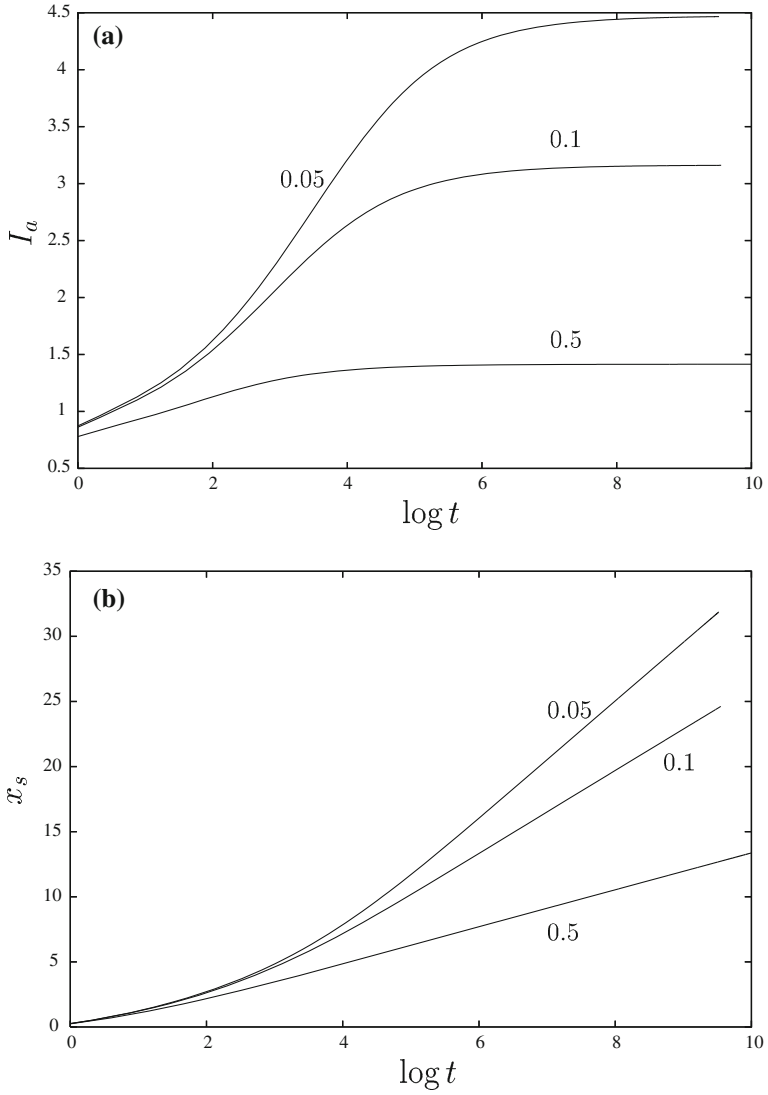

Fig. 5 *Plots* of **a** the amount of A formed I_a, **b** the position of the reaction zone x_s against $\log t$ for $\delta = 1.0$, $\beta = 0.05,\ 0.1,\ 0.5$ and $D = 0$

plot x_s against $\log t$ in Fig. 5b for the same parameter values. We see that the curves have a constant slope, again dependent on β, at large times. This indicates that x_s is of $O(\log t)$ for t large.

3.2.1 Asymptotic solution for **t** *large*

As t increases the concentration of A approaches a steady state $a = a(x)$ and a front in the reactant B propagates slowly across the region. From Eq. (8) with $b = 0$ and boundary conditions (10),

$$a(x) = \mathrm{e}^{-\sqrt{\beta}\,x} \quad \text{as } t \to \infty \tag{22}$$

and then, from equation (9)

$$b = \exp(-t\,\mathrm{e}^{-\sqrt{\beta}\,x}) \tag{23}$$

Note that this solution has $b \to 0$ as $t \to \infty$ for any finite x. To obtain more information about the propagating front in B we note that (23) has $b \simeq 0$ up to where

$$t\,\mathrm{e}^{-\sqrt{\beta}x} \text{ is } O(1), \quad \text{or} \quad x \sim \frac{1}{\sqrt{\beta}}\log t \tag{24}$$

This suggests that we put

$$x = \frac{1}{\sqrt{\beta}}\log t + \xi, \quad \xi \text{ of } O(1) \tag{25}$$

for the propagating front, with (22, 23) then giving

$$b = \exp(-\mathrm{e}^{-\sqrt{\beta}\,\xi}), \quad a = t^{-1}\,\mathrm{e}^{-\sqrt{\beta}\,\xi} \tag{26}$$

In (26) $b \to 0$ as $\xi \to -\infty$ and $b \to 1$ as $\xi \to \infty$.

Expressions (26) suggest that for this front region we put $a = t^{-1}\,F(\xi, t)$, leaving b unscaled. If we substitute this and expression (25) into Eqs. (8, 9) with $D = 0$ and look for a solution by expanding in inverse powers of t, we find that the leading-order terms $(F_0(\xi),\ b_0(\xi))$ satisfy

$$F_0'' - \delta F_0 b_0 - \beta F_0 = 0, \quad b_0' - \sqrt{\beta}\,F_0 b_0 = 0 \tag{27}$$

subject to the conditions in (26) as $\xi \to -\infty$, and with $F_0 \to 0,\ b_0 \to 1$ as $\xi \to \infty$, where primes now denote differentiation with respect to ξ. We can combine Eqs. (27) if we put $\psi = -\displaystyle\int_{\xi}^{\infty} F_0(y)dy$, then

$$b_0 = \mathrm{e}^{\sqrt{\beta}\,\psi}, \quad \psi'' + \frac{\delta}{\sqrt{\beta}}(1 - \mathrm{e}^{\sqrt{\beta}\,\psi}) - \beta\psi = 0 \tag{28}$$

We can solve Eq. (28) for ψ subject to

$$\psi \to 0 \ \text{ as } \xi \to \infty, \quad \psi' \sim \mathrm{e}^{-\sqrt{\beta}\xi} \ \text{ as } \xi \to -\infty \tag{29}$$

and hence calculate b_0. A plot of $b_0(\xi)$ is given in Fig. 6 for $\beta = 0.05$ and $\beta = 0.5$, showing that the spread of the reaction front decreases as β is increased, as might be expected from (26).

From our analysis $I_a \to \beta^{-1/2}$ as $t \to \infty$ consistent with the asymptotic values seen in Fig. 5a. We note that this asymptotic result is independent of δ, as might be

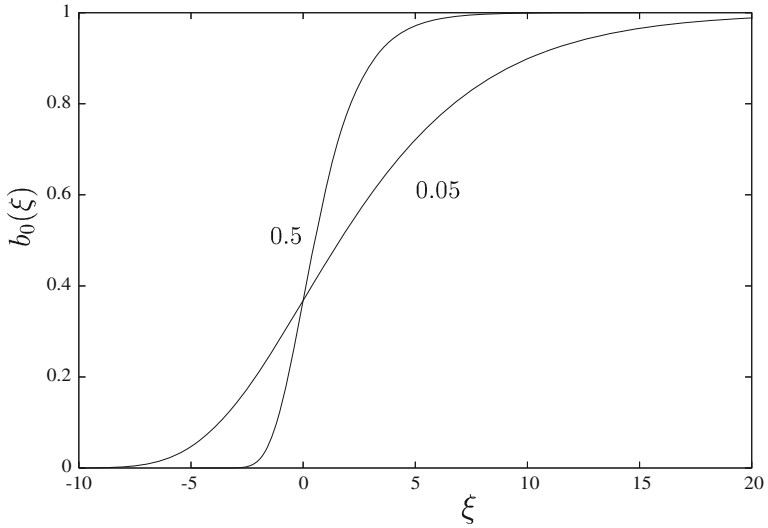

Fig. 6 Plots of $b_0(\xi)$ determined by (28, 29) for $\beta = 0.05,\ 0.5$

expected since this steady state in A is really a balance between the diffusive spread of A from the boundary and its decay through reaction (2). From (25)

$$x_s \sim \frac{1}{\sqrt{\beta}} \log t \quad \text{as } t \to \infty \tag{30}$$

Expression (30) shows that the slope of the plots of x_s against $\log t$ shown in Fig. 5b should have a slope of $\beta^{-1/2}$, as appears to be the case for these plots.

4 Complexing agent able to diffuse, D > 0

We now assume that the reactant B is free to diffuse, though more slowly than the reactant A. Thus we take only relatively small values for the diffusion coefficient ratio D. As before we start by considering the case when there is no degradation of the reactant B.

4.1 No reactant degradation, $\boldsymbol{\beta = 0}$

The situation in this case is similar to the previous case when the reactant B was immobile. We illustrate this in Fig. 7a where we give profile plots of A and B for $D = 0.1$ and $\delta = 1.0$ to compare with Fig. 1. Again we see that there is a region near the wall where the concentration of A decreases almost linearly and in which $b = 0$. There is a relatively thin reaction zone where the concentrations of both A and B are small and a final region where the concentration of A is zero and the concentration of B increases to its outer state, $b = 1$. The only difference between the two cases,

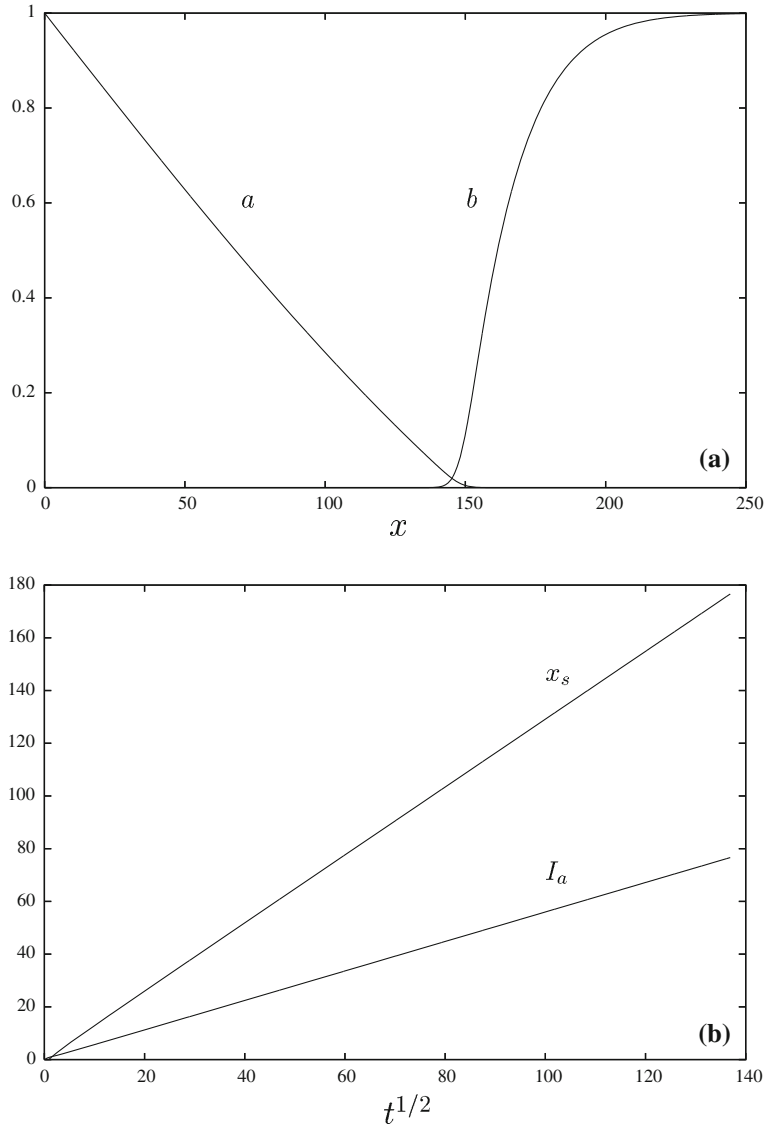

Fig. 7 **a** Concentration profiles of A and B calculated from a numerical integration of equations (8, 9) subject to (10, 11) for $D = 0.1$, $\delta = 1.0$, $\beta = 0.0$ at time $t = 18481.8$. **b** *Plots* of the position of the reaction x_s and the amount of A formed I_a against $t^{1/2}$

Figs. 1 and 7a, is that the spread of the concentration of B in the final region is a little greater when B is allowed to diffuse. Again the concentration of A spreads from the wall at a rate of $O(t^{1/2})$ for t large. We illustrate this in Fig. 7b with plots of x_s and I_a against $t^{1/2}$, both showing a constant slope for t large. If we compare the slopes of the plots in Figs. 2 and 7b, we find that they are very similar. This suggests that the

reactant A and the reaction zone moves away from the wall at about the same rate in both cases, at least for this value of δ.

4.1.1 Asymptotic solution for **t** *large*

In this case we find that there is a three-region structure to the solution for t large. There is an inner (diffusive) region as before where $b = 0$ and the solution for a is given by (12–15). There is an outer (again diffusive) region where $a = 0$ and in which we put $\overline{\eta} = \overline{x}/c(t)$, where $\overline{x}$ is defined in (16) and $c(t)$ in (13). Equation (9) then gives

$$D\,\frac{\partial^2 b}{\partial \overline{\eta}^2} + (\overline{\eta}+1)c\dot{c}\,\frac{\partial b}{\partial \overline{\eta}} = \frac{\partial b}{\partial t} \tag{31}$$

The leading-order problem is

$$Db_0'' + 2c_0^2(\overline{\eta}+1)b_0' = 0 \quad b_0 \to 1 \text{ as } \overline{\eta} \to \infty \tag{32}$$

where primes now denote differentiation with respect to $\overline{\eta}$. We solve (32) subject to the condition that $b_0 = 0$ at $\overline{\eta} = 0$, i.e. at $x = c(t)$ to leading order. Thus

$$b_0(\overline{\eta}) = 1 - \frac{1}{I_1}\int_{\overline{\eta}}^{\infty} \mathrm{e}^{-c_0^2(s^2+2s)/D}\,ds \tag{33}$$

where

$$I_1(c_0, D) = \int_0^{\infty} \mathrm{e}^{-c_0^2(s^2+2s)/D}\,ds = \frac{\sqrt{D}\,\mathrm{e}^{c_0^2/D}}{c_0}\int_{c_0/\sqrt{D}}^{\infty} \mathrm{e}^{-s^2}\,ds$$

From (33),

$$b \sim \frac{1}{I_1}\,\overline{\eta} + \cdots = \frac{t^{-1/2}}{2c_0 I_1}\,\overline{x} + \cdots \quad \text{for } \overline{x} \text{ small} \tag{34}$$

A central (reaction) region is required which matches with both the outer and inner regions and in which reaction (1) has a significant effect. For this region we put

$$a = t^{-1/3}\,F(\zeta), \quad b = t^{-1/3}\,G(\zeta), \quad \zeta = \overline{x}\,t^{-1/6} \tag{35}$$

Applying (35) in Eqs. (8, 9) gives

$$\frac{\partial^2 F}{\partial \zeta^2} - \delta FG = \frac{\partial F}{\partial t} - t^{-2/3}\left(\frac{1}{3}\,F + \frac{1}{6}\,\zeta\,\frac{\partial F}{\partial \zeta}\right) - t^{-1/3}\,(c_0 + \cdots)\,\frac{\partial F}{\partial \zeta} \tag{36}$$

$$D\frac{\partial^2 G}{\partial \zeta^2} - FG = \frac{\partial G}{\partial t} - t^{-2/3}\left(\frac{1}{3}\,G + \frac{1}{6}\,\zeta\,\frac{\partial G}{\partial \zeta}\right) - t^{-1/3}\,(c_0 + \cdots)\,\frac{\partial G}{\partial \zeta} \tag{37}$$

subject to, from (18) and (34),

$$F \sim -\frac{d_0}{2c_0}\,\zeta + \cdots,\ G \to 0 \text{ as } \zeta \to -\infty,$$
$$F \to 0,\ G \sim \frac{1}{2c_0 I_1}\,\zeta + \cdots \text{ as } \zeta \to \infty \tag{38}$$

The leading-order problem is

$$F_0'' - \delta F_0 G_0 = 0, \quad D G_0'' - F_0 G_0 = 0 \tag{39}$$

subject to (38) and where primes denote differentiation with respect to ζ. Combining the equations in (39), integrating and applying the boundary condition as $\zeta \to -\infty$ gives

$$F_0' - D\delta G_0' = -\frac{d_0}{2c_0} \tag{40}$$

Now applying the condition in (38) as $\zeta \to \infty$ leads to

$$-\frac{D\delta}{2c_0 I_1} = -\frac{d_0}{2c_0} \quad \text{or} \quad \delta = \frac{\mathrm{e}^{-c_0^2} I_1}{D I_0} \tag{41}$$

It is relation (41) that determines c_0 implicitly in terms of δ. We note that $I_1 \sim \dfrac{D}{2c_0^2}$ for D small and applying this in (41) we recover (21) as $D \to 0$. We plot c_0 against δ obtained from expression (41) in Fig. 8 for a range of values of D. There is very little difference in the values of c_0 for the smaller values of δ, it is only for the larger values of δ that any real difference is seen as the value of D is changed. We note that, for $D = 0.1$ and $\delta = 1.0$, we find a value for c_0 of 0.5936 close the value quoted above when $D = 0$. This provides the reason why we found in our numerical integrations that the spread of the reaction region was similar in both these cases.

4.2 Reactant degradation, $\boldsymbol{\beta \neq 0}$

We illustrate this case with plots of the concentrations of A and B in Fig. 9a for $\beta = 0.5$, $D = 0.1$, $\delta = 1.0$ to compare with Fig. 4 for $D = 0$. We highlight the reaction region, where the concentrations of A and B are nonzero, in Fig. 9b. As before the concentration of A approaches a steady state as t increases and remains attached to the wall. We show this in Fig. 10a with plots of I_a against $\log t$ for representative values of β. As previously our numerical results indicate that the spread of A from the wall increases as the value of β is decreased. In this region near the wall where A decreases to zero, the concentration of B reduces to zero. If we compare Fig. 9a with Fig. 4 we see that the spread of B is much greater, more diffusive, for $D = 0.1$ than for $D = 0$. However, we find a difference with the previous, $D = 0$, case in that the

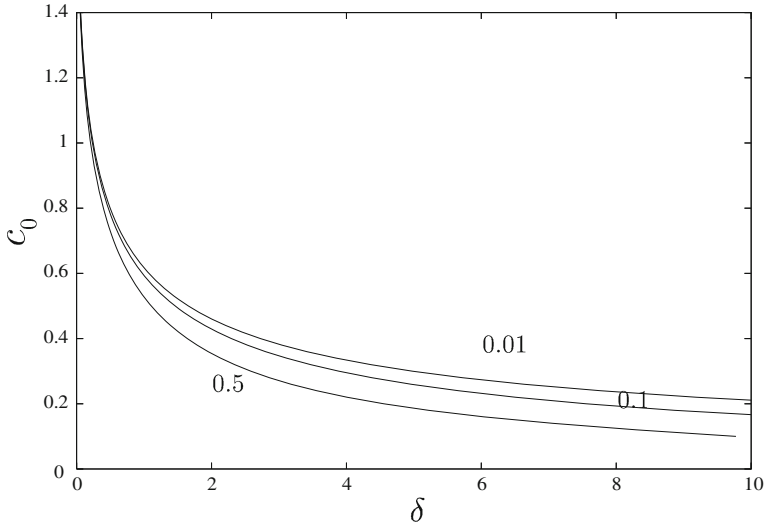

Fig. 8 *Plots* of c_0 against δ given by Eq. (41) for $D = 0.01,\ 0.1,\ 0.5$, the position of the reaction zone $x_s \sim 2c_0 t^{1/2}$ for t large

spread of x_s, the position where $b = 0.5$, is no longer logarithmic with t, as seen in Fig. 5b, but appears to increase like $t^{1/2}$. We show this in Fig. 10b with plots of x_s against $t^{1/2}$ for different values of β, with the curves becoming straight lines for the larger values of t. This $t^{1/2}$ spread is perhaps to be expected as the values of x_s are calculated in the region where $a = 0$ and B is purely diffusing.

If we examine how the reaction zone evolves in more detail we find that initially it spreads from the wall as the concentration of B decreases there. However, for very large times the region where the concentrations of both A and B are nonzero appears to reach a constant position, not spreading any further from the wall, unlike the $D = 0$ case where a definite, though slow, spread of the reaction zone can clearly be seen in the numerical simulations.

4.2.1 Asymptotic solution for **t** *large*

For large times the structure of the solution consists of an inner region of $O(1)$ thickness where a reaches a steady state and a much thicker outer region of $O(t^{1/2})$ thickness, see Fig. 10b, where $a = 0$ and B spreads purely by diffusion. In this outer region Eq. (9) reduces to the diffusion equation which then has the solution

$$b = 1 - \frac{1}{\sqrt{\pi D}} \int_{\eta}^{\infty} \mathrm{e}^{-s^2/4D}\, ds \quad \text{where } \eta = \frac{x}{t^{1/2}} \tag{42}$$

on satisfying the condition that $b = 0$ at $x = 0$ (the inner edge of the outer region). From (42)

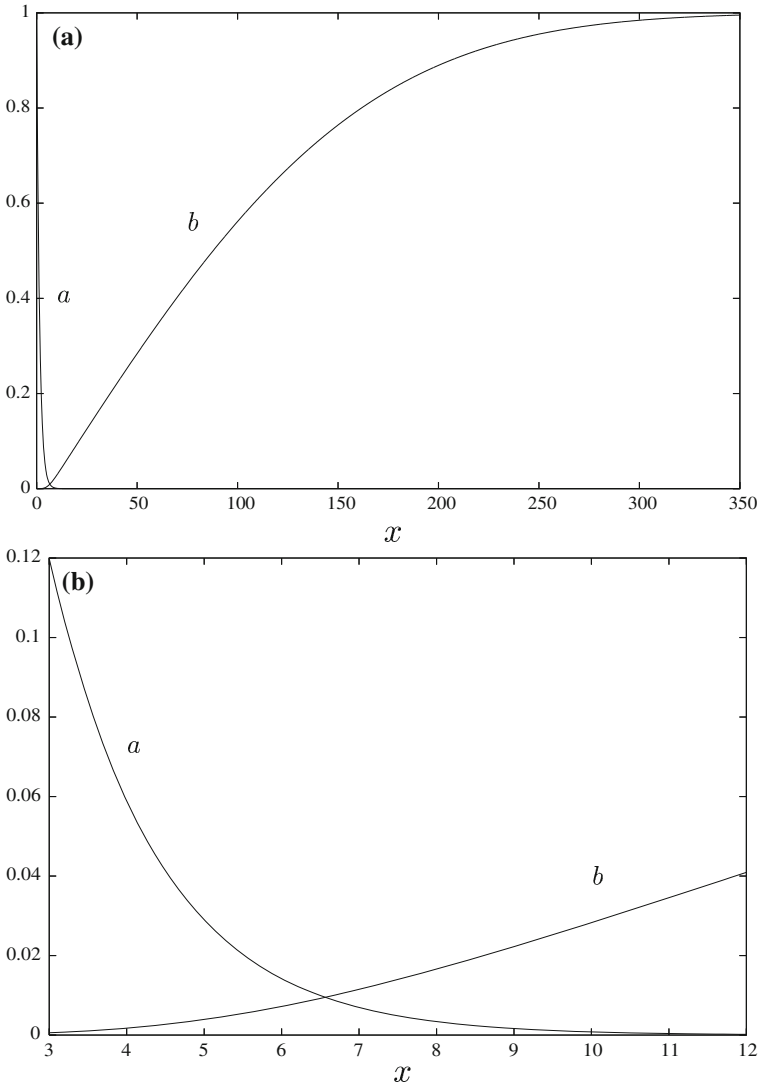

Fig. 9 **a** Concentration profiles of A and B, **b** with an *inset* to show the reaction zone, calculated from a numerical integration of equations (8, 9) subject to (10, 11) for $D = 0.1$, $\delta = 1.0$, $\beta = 0.5$ at time $t = 74{,}236$

$$b \sim \frac{x}{\sqrt{\pi D}}\, t^{-1/2} + \cdots \quad \text{for } x \text{ small} \tag{43}$$

Expression (43) indicates that for the inner region we have, at leading order,

$$a \to \mathrm{e}^{-\sqrt{\beta}x}, \quad b = t^{-1/2}\, G(x) \tag{44}$$

where G satisfies

$$DG'' - \mathrm{e}^{-\sqrt{\beta}x}\, G = 0, \quad G'(0) = 0, \; G \sim \frac{x}{\sqrt{\pi D}} \text{ as } x \to \infty \tag{45}$$

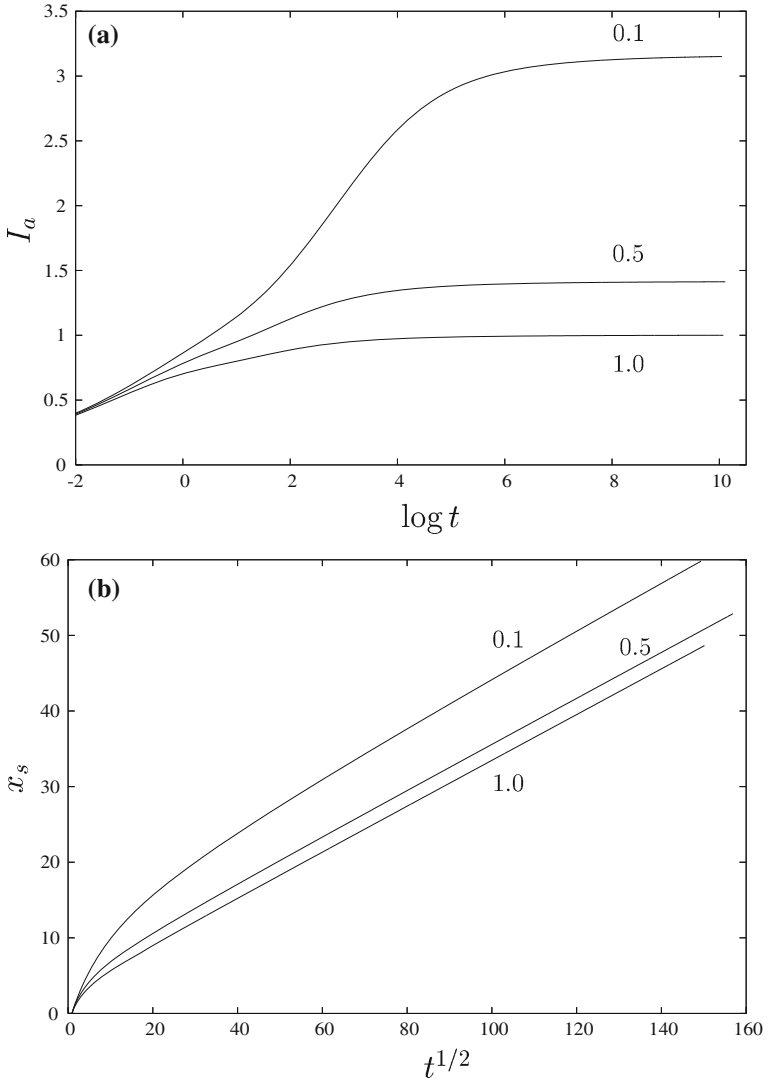

Fig. 10 **a** The amount of A formed I_a plotted against $\log t$, **b** the position of the reaction x_s plotted against $t^{1/2}$ for $D = 0.1$, $\delta = 1.0$, $\beta = 0.1,\ 0.5,\ 1.0$

Equation (45) can be solved in terms of Bessel functions [18] by writing $y = \dfrac{2}{\sqrt{\beta D}}\,\mathrm{e}^{-\sqrt{\beta}x/2}$ to obtain

$$G'' + \frac{1}{y}\,G' - G = 0 \tag{46}$$

subject to

$$G' = 0 \text{ at } y = \frac{2}{\sqrt{\beta D}}, \quad G \sim -\frac{2\log y}{\sqrt{\beta D\pi}} + \cdots \text{ as } y \to 0 \tag{47}$$

where primes now denote differentiation with respect to y. Equation (46) has the solution

$$G(y) = \frac{2}{\sqrt{\beta D\pi}} \left(K_0(y) + \frac{K_1(y_0)}{I_1(y_0)} I_0(y) \right) \quad \text{where } y_0 = \frac{2}{\sqrt{\beta D}} \tag{48}$$

From (45) we see that the reaction (1) between A and B plays no part, at least to leading order, in the large time development of the solution. In fact, as in the previous case when $D = 0$, the large time structure is mainly the interaction between the diffusive spread of A from the boundary and its degradation through reaction (2), the depletion of A and B near the boundary through reaction (1) being a second-order effect.

The form of the concentration profile for B seen in Fig. 9 is apparent from expression (48). For the parameter values used for Fig. 9, $y_0 \simeq 8.944$ and, if we use the asymptotic expressions for the Bessel functions in (48), the ratio $K_1(y_0)/I_1(y_0) \sim \mathrm{e}^{-2y_0}/\pi \simeq 5.42 \times 10^{-9}$ and can effectively be neglected. Thus, on the boundary $x = 0$ (or $y = y_0$), $G \sim \dfrac{2\sqrt{2}}{\pi\sqrt{\beta D y_0}}\, \mathrm{e}^{-y_0} \simeq 2.97 \times 10^{-4}$. It is only at the outer edge of this inner region with y close to zero that G takes $O(1)$ values.

5 Conclusions

We have considered a basic reaction scheme whereby two species A and B (say) react to form an inert product AB, reaction (1). We also include in our scheme the possible linear decay of reactant A, reactant (2). With B present initially at a uniform concentration and A being maintained at a constant concentration on the boundary, propagating reaction–diffusion structures can develop in which B is totally consumed. Perhaps the simplest and most robust of these reaction fronts is seen when there is only the reaction (1) between A and B with B immobile. In this case a 'sharp' front in B is seen which propagates from the boundary, see Figs. 1 and 2. Although the front in B shown in Fig. 1 is similar in form to other travelling wave structures, for example in [5,4,7], in that it has an $O(1)$ thickness, it propagates at a rate proportional to $t^{1/2}$ whereas the propagation speed of autocatalytic travelling waves is of $O(t)$, for t large.

This situation is in many ways the same when B is allowed to diffuse (though, as part of our modelling assumptions, at a much slower rate than A), see Fig. 7a. The differences between this case and when B is immobile is that the reaction front in B appears less 'sharp' and has an outer region in which there is a diffusive spread of B from its depleted value in the reaction zone to its outer, initial input value. Though perhaps a more important difference is seen in the width of the reaction front which now has an increasing thickness, being of $O(t^{1/6})$ for t large, see expression (35), whereas previously it remained of $O(1)$.

When we also allow for the decay of reactant A via reaction (2), we again see a propagating reaction front in B develop when B is immobile, see Fig. 4. However, here the interplay between the reactants A and B is perhaps more subtle. Reaction B is totally consumed near the boundary leaving only the decay of A through reaction (2)

and the input of A from the boundary. The result is that, with $b = 0$, the concentration of A reaches a steady state, as given in (22). However, the exponentially small values of a at the edge of this region are sufficient to generate a reaction with B leading to further depletion of B through reaction (1) and to the slow propagation of a reaction front in B. As a consequence of the concentration of A being exponentially small at the inner edge of this reaction front, it propagates at a rate of $O(\log t)$, see (30), thus needing much greater times than previously to advance from the boundary. As a check that it was these exponentially small concentrations of A that were responsible for setting up the front in B, we artificially put a to zero when it had reached a sufficiently small value in our numerical simulations. Again a reaction front similar to that shown in Fig. 4 was set up, though after a while it stopped propagating when it reached the point where we had put a to zero.

The final case that we considered was when B could diffuse and there was decay of reactant A. Now the system evolved to give finally a constant profile for a with b being small, of $O(t^{-1/2})$, in the reaction region, expressions (44, 48). There is also an outer region, purely diffusive region in B, see Fig. 9. At least for the smaller values of D considered here, the solution evolves to form a structure close to the boundary where the concentration of B is virtually zero, the thickness of this region being of $O(D^{-1/2})$ from expression (48).

In our numerical integrations we applied a zero flux boundary condition on B at the boundary $x = 0$. This condition is not particularly significant. We also performed some numerical integrations applying the condition that $b = 0$ at $x = 0$. Though the initial development of the solution in this case had some differences with the previous (zero flux) results, the large time structures were essentially the same. This perhaps should be expected as we have seen the concentration of B becomes virtually zero in all the cases we hve discussed.

References

1. R.A. Fisher, The wave of advance of advantageous genes. Ann. Eugenics **7**, 353–369 (1937)
2. A. Kolmogorov, I. Petrovski, N. Piscounov, Etude de l'équation de la diffusion avec crissance de la quantité de maitière et son application à une probléme biologique. Mosc. Univ. Bull. Math. **1**, 1–25 (1937)
3. A. Saul, K. Showalter, Propagating reaction–diffusion fronts, in *Oscillations and Travelling Waves in Chemical Systems*, ed. by R.J. Field, M. Burger (Wiley, New York, 1984)
4. J. Billingham, D.J. Needham, The development of travelling waves in quadratic and cubic autocatalysis with unequal diffusion coefficients. I. Permanent form travelling waves. Phil. Trans. R. Soc. Lond. A **334**, 1–24 (1991)
5. K. Showalter, Quadratic and cubic reaction–diffusion fronts. Nonlinear Sci. Today **4**, 1–10 (1995)
6. J.H. Merkin, D.J. Needham, Reaction–diffusion in an isothermal chemical system with general orders of autocatalysis and spatial dimension. J. Math. Phys. (ZAMP) **44**, 707–721 (1993)
7. J.H. Merkin, D.J. Needham, The development of travelling waves in a simple isothermal chemical system. II Cubic autocatalysis with quadratic and linear decay. Proc. Roy. Soc. Lond. A **430**, 315–345 (1990)
8. D.J. Needham, J.H. Merkin, The development of travelling waves in a simple isothermal chemical system with general orders of autocatalysis and decay. Phil. Trans. Roy. Soc. Lond. A **337**, 261–274 (1991)
9. R.J. Field, M. Burger (eds.) *Oscillations and Traveling Waves in Chemical Systems* (Wiley, New York, 1987)

10. S.K. Scott, *Oscillations, Waves and Chaos in Chemical Kinetics* (Oxford University Press, Oxford, 1994)
11. R. Kapral, K. Showalter (eds.) *Chemical Waves and Patterns* (Kluwer, Dordrecht, 1995)
12. R. Aris, *The mathematical theory of diffusion and reaction in permeable catalysts. I The theory of the steady state* (Clarendon Press, Oxford, 1975)
13. R. Aris, *The mathematical theory of diffusion and reaction in permeable catalysts. II Questions of uniqueness, stability and transient behaviour* (Clarendon Press, Oxford, 1975)
14. J.H. Merkin, H. Ševčíková, The effects of a complexing agent on travelling waves in autocatalytic systems with applied electric fields. IMA J. Appl. Math. **70**, 527–549 (2005)
15. J.H. Merkin, D.J. Needham, Propagating reaction–diffusion waves in a simple isothermal autocatalytic chemical system. J. Eng. Math. **23**, 343–356 (1989)
16. J.H. Merkin, H. Ševčíková, D. Šnita, The effect of an electric field on the local stoichiometry of front waves in an ionic chemical system. IMA J. Appl. Math. **64**, 157–188 (2000)
17. D.J. Needham, J.A. Leach, J.H. Merkin, The effects of a complexation reaction on travelling wavefronts in a quadratic autocatalytic system. Q. J. Mech. Appl. Math. **58**, 577–599 (2005)
18. G.N. Watson, *A Treatise on the Theory of Bessel Functions* (Cambridge University Press, Cambridge, 1966)